J. Phys. B: At. Mol. Opt. Phys. **31** (1998) 4427–4436. Printed in the UK PII: S0953-4075(98)89782-4

Ps–H scattering using a projectile elastic close-coupling approximation

H Ray and A S Ghosh

Department of Theoretical Physics, Indian Association for the Cultivation of Science, Jadavpur, Calcutta—700032, India

Received 4 December 1997, in final form 12 May 1998

Abstract. A projectile elastic close-coupling approximation with electron exchange is employed to study Ps–H scattering using the basis set [Ps(1s) + H(1s, 2s, 2p)] at low and medium energies. The s-, p- and d-wave phase shifts are reported below 5.1 eV along with the integrated cross sections for elastic (also quenching) and target inelastic transitions. The present prediction is compared with other theoretical predictions and found to be consistent. The conversion ratio approaches the value 0.25 with the increase of incident Ps energy.

1. Introduction

Recently the scattering of the positronium (Ps) atom off atomic/molecular targets has been studied both experimentally and theoretically. Very recently measurements of Ps–gas total cross sections for He, Ar, H_2 and O_2 have been made by Laricchia and co-workers (Zafar *et al* 1994, Gerner and Laricchia 1996, Ozen *et al* 1997) at medium energies. Ozen *et al* (1997) pointed out that their measurements have highlighted the importance of electron exchange between the Ps and target electrons at low energies and also target inelastic processes at medium and high energies.

The importance of electron exchange in Ps–gas scattering at low energies is evident from the theoretical studies carried out by Hara and Fraser (1975), Drachman and Houston (1975), and Ray and Ghosh (1996, 1997) for Ps–H scattering and by Fraser and Kraidy (1966), Barker and Bransden (1968) and Sarkar and Ghosh (1997) for Ps–He scattering. McAlinden *et al* (1996) have investigated the scattering of Ps atoms off gas target atoms using the target elastic Ps pseudostate close-coupling approximation (CCA) in which the target always remained in its initial state. In their basis set a few low-lying eigenstates and some pseudostates of Ps atom are taken into account. In their investigation, they did not consider electron exchange. They reported the results of Ps–He and Ps–Ar scattering. They noticed that for light target atoms, target inelastic collision becomes dominant at intermediate energies. In our previous paper (Sinha *et al* 1997), we investigated the target elastic Ps CCA to study Ps–H scattering using the basis set:

$$\mathrm{H(1s)} + \mathrm{Ps(1s, 2s, 2p)}$$

including electron exchange. It has been found that the results at low energies are modified appreciably. The findings of McAlinden *et al* (1996) and measurements indicate that the calculation including inelastic channel of the target atom is warranted. The motivation of this paper is to estimate the effect of the excited state of the target atom on the elastic

0953-4075/98/194427+10$19.50

channel and also to provide a reasonable estimate of the target inelastic processes using the close-coupling method.

In this study, we employ projectile elastic CCA to investigate Ps–H scattering. In this calculation, the projectile Ps atom always remains in the ground state. The exchange of electrons between Ps and H atoms is included by properly antisymmetrizing the total wavefunction of the system. We employ the following basis set:

$$\mathrm{H(1s,\ 2s,\ 2p) + Ps(1s).}$$

It may be mentioned that for all transitions in which the Ps atom always remains in the ground state, the direct first Born approximation (FBA) cross sections vanish. In other words the scattering amplitude obtained by using projectile elastic CCA neglecting exchange does not exist. The surviving FBA amplitudes are due to exchange interaction. The s-, p- and d-wave phase shifts are reported below 5.1 eV using CCA. We also report integrated cross sections for elastic (also quenching) and target inelastic transitions in the energy range from 0–200 eV.

2. Theory

The total wavefunction of the system comprising Ps and H atoms may be written as

$$\Psi^{\pm}(r_p, r_1, r_2) = \frac{1}{\sqrt{2}}(1 \pm P_{12}) \sum_n \Phi_n(r_2)\eta_{1s}(\rho_1)F_n(R_1) \tag{1}$$

where P_{12} stands for the exchange operator and $R_i = \frac{1}{2}(r_p + r_i)$ and $\rho_i = r_p - r_i; i = 1, 2$. Here the position vectors of the two electrons belonging to the Ps and H atoms are denoted by r_1 and r_2 respectively and r_p, that of positron with respect to the centre of mass of the system which lies with the proton. In expansion (1), we assume that the Ps atom will not be excited during collision. The explicit dependence of the spin function has not been taken into account and the scattering parameters will finally be obtained by proper spin averaging.

Here $\Phi_n(r)$ and $\eta_{1s}(\rho)$ are the wavefunctions of the H and Ps atoms respectively and $F_n(R)$ is the continuum wavefunction of the Ps atom. The total Hamiltonian of the system may be expressed as

$$H = -\frac{1}{2}\nabla_p^2 - \frac{1}{2}\nabla_1^2 - \frac{1}{2}\nabla_2^2 + \frac{1}{r_p} - \frac{1}{r_1} - \frac{1}{r_2} - \frac{1}{|r_p - r_1|} - \frac{1}{|r_p - r_2|} + \frac{1}{r_1 - r_2}. \tag{2}$$

The total wavefunction must satisfy the Schrödinger equation

$$H\Psi^{\pm}(r_p, r_1, r_2) = E\Psi^{\pm}(r_p, r_1, r_2). \tag{3}$$

The formally exact Lippman–Schwinger-type coupled integral equations for scattering amplitude in momentum space are given by (Basu *et al* 1989, Sinha *et al* 1997)

$$f^{\pm}_{n'1s,n1s}(\vec{k}', \vec{k}) = B_{n'1s,n1s}(\vec{k}', \vec{k}) - \frac{1}{2\pi^2}\sum_{n''}\int \mathrm{d}\vec{k}'' \frac{B^{\pm}_{n'1s,n''1s}(\vec{k}', \vec{k}'')f^{\pm}_{n''1s,n1s}(\vec{k}'', \vec{k})}{k^2_{n''1s} - k''^2 + \mathrm{i}\varepsilon}. \tag{4}$$

It may be noted that $B^{\pm}$ stands for the first Born and Born–Oppenheimer (B–O) scattering amplitudes (see Sinha *et al* 1997).

After partial wave analysis, the three-dimensional coupled integral equations (equation (4)) reduce to one-dimensional coupled integral equations (Basu *et al* 1989). Two sets of coupled one-dimensional integral equations, one corresponding to f_L^+ and the other to f_L^-, are solved numerically by the matrix inversion method for each partial wave. The scattering parameters are obtained from standard relations (Fraser 1962).

3. Results and discussion

To solve the two sets of one-dimensional integral equations, we have to evaluate the B–O scattering amplitudes for different processes. The B–O amplitudes are evaluated in two ways as a check of the program. Moreover, the values of integrated B–O cross sections evaluated by partial wave and non-partial wave methods are found to be identical. This assures that the partial wave analysis is correct.

The two sets of one-dimensional integral equations are solved numerically. The pole term is replaced by delta function and principal value parts:

$$\frac{1}{k_n^2 - k''^2 + \mathrm{i}\varepsilon} = -\mathrm{i}\pi\delta(k_n^2 - k''^2) + \frac{P}{k_n^2 - k''^2}.$$

Using the Gaussian quadrature method we have obtained a set of simultaneous equations for both f_L^+ and F_L^-, that have been solved by the matrix inversion method. The principal value integral from zero to infinity has been replaced by

$$\int_0^\alpha = \int_0^{2k_n} + \int_{2k_n}^\alpha .$$

We have used an even number of Gaussian points in the interval 0–$2k_n$ so that the limit $k'' = k_n$ has been taken from both sides. By increasing the number of Gaussian points we have tested the convergence of the amplitudes. It may be mentioned that the rate of convergence is very slow at low energies. In actual calculations, we have taken 32 and 16 points in the intervals $(0$–$2k_n)$ and $(2k_m$–$\alpha)$ respectively.

In calculation, we solve the coupled integral equations up to angular momentum $\boldsymbol{I} = 7$ for the lowest energy (i.e. 0.068 eV) while this is increased to $\boldsymbol{I} = 20$ for the highest energy (i.e. 200 eV) considered. At intermediate energies the number of partial waves is adjusted proportionately. The contributions of the higher angular momenta to the integrated cross sections are replaced by the partial wave first Born contributions.

Table 1 represents the present CCA s-wave (singlet and triplet) phase shifts in the energy range 0.01–0.64 Ryd. The static exchange (Ray and Ghosh 1997) and the target elastic CCA (Sinha *et al* 1997) predictions are compared with those of present results. The singlet phase shifts obtained by the projectile elastic CCA differ (figure 1) significantly from those of the static exchange method in the energy range considered, the present predictions being always

Table 1. The s-wave phase shifts in radians for [Ps(1s) + H(1s)] scattering.

	Results using static exchange method		Results using three-state exchange target elastic CCA		Results using three-state exchange projectile elastic CCA	
k (au)	Singlet (η_0^+)	Triplet (η_0^-)	Singlet (η_0^+)	Triplet (η_0^-)	Singlet (η_0^+)	Triplet (η_0^-)
0.1	2.45	2.89	2.46	2.90	2.55	2.90
0.2	1.93	2.65	1.94	2.67	2.05	2.66
0.3	1.55	2.42	1.55	2.45	1.66	2.43
0.4	1.24	2.20	1.25	2.25	1.35	2.22
0.5	1.00	2.00	1.01	2.06	1.11	2.02
0.6	0.78	1.81	0.82	1.91	0.90	1.83
0.7	0.63	1.64	0.66	1.78	0.73	1.67
0.8	0.49	1.49	0.54	1.74	0.58	1.51

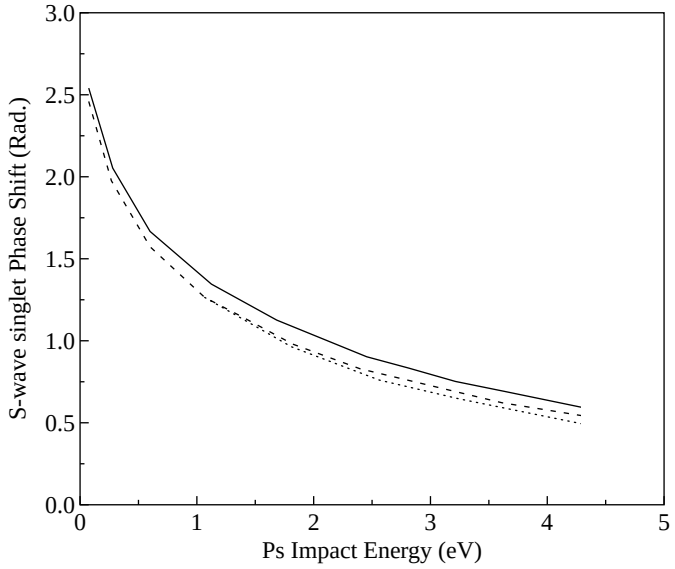

Figure 1. The s-wave elastic singlet phase shifts in radians. —— present results; - - - - Sinha *et al* (1997); ····· static exchange, Ray and Ghosh (1997).

higher. On the other hand, the difference between the present and static exchange triplet phase shifts is marginal in this energy range (figure 2). In contrast, the target elastic CCA (Sinha *et al* 1997) singlet phase shifts are very close to those of static exchange whereas the triplet phase shifts of target elastic CCA differ from those of static exchange with increase of energy. In the case of singlet phase shifts, the target elastic CCA prediction lies between the corresponding phase shifts obtained by using the projectile elastic CCA and the static exchange method. Whereas in the case of triplets the present curve lies between the other two.

The inclusion of the 2p-state of the target atom in the expansion scheme introduces a long-range dipole correlation potential in a dynamic way. This potential is attractive in nature and is responsible for the enhancement of the s-wave singlet phase shift in Ps–H scattering. The literature reveals that induced dipole interaction influences the elastic low-order singlet phase shifts significantly (Burke *et al* 1963). On the other hand, a triplet phase shift is less sensitive to long-range interaction. The marginal change in the present triplet phase shift from that of the static exchange model is thus understood. This feature has also been noticed in the case of electron–hydrogen scattering (Burke *et al* 1963). The long-range attractive interaction as induced by the present model partially reduces the repulsive exchange interaction. In the target elastic close-coupling model as employed by Sinha *et al*, the coupling effect also partially reduces the repulsive exchange interaction. Sinha *et al* have noticed that their elastic s-wave triplet phase shift is influenced appreciably whereas there is marginal change in the case of singlet when compared with static exchange prediction. This indicates that the inclusion of the 2p-state of the projectile atom in the expansion scheme gives rise to a short-range attractive potential.

The present p- and d-wave phase shifts up to the incident positronium energy 0.64 Ryd are tabulated in tables 2 and 3, respectively. These tables also contain the corresponding predictions of the static exchange model and the target elastic CCA. As in the case of s-wave, the present singlet p- and d-wave phase shifts differ appreciably from those of

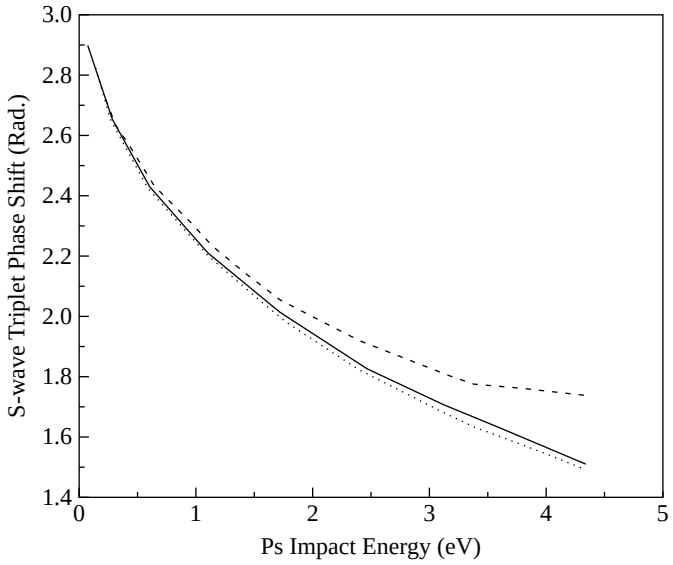

Figure 2. The s-wave elastic triplet phase shifts in radians. —— present results: - - - - Sinha *et al* (1997); ····· static exchange, Ray and Ghosh (1997).

Table 2. The p-wave phase shifts in radians for [Ps(1s) + H(1s)] scattering. The numbers in parentheses indicate the power of '10'.

	Results using static exchange method		Results using three-state exchange target elastic CCA		Results using three-state exchange projectile elastic CCA	
k (au)	Singlet (η_1^+)	Triplet (η_1^-)	Singlet (η_1^+)	Triplet (η_1^-)	Singlet (η_1^+)	Triplet (η_1^-)
0.1	7.98(−3)	−5.03(−3)	8.14(−3)	−4.43(−3)	8.95(−3)	−4.59(−3)
0.2	6.14(−2)	−3.52(−2)	6.27(−2)	−3.08(−2)	6.97(−2)	−3.22(−3)
0.3	1.88(−1)	−9.80(−2)	1.90(−1)	−8.51(−2)	2.13(−1)	−9.03(−2)
0.4	3.49(−1)	−1.86(−1)	3.58(−1)	−1.59(−1)	4.00(−1)	−1.72(−1)
0.5	4.77(−1)	−2.87(−1)	4.89(−1)	−2.36(−1)	5.43(−1)	−2.67(−1)
0.6	5.36(−1)	−3.90(−1)	5.51(−1)	−3.02(−1)	6.03(−1)	−3.63(−1)
0.7	5.38(−1)	−4.88(−1)	5.56(−1)	−3.32(−1)	6.02(−1)	−4.54(−1)
0.8	5.08(−1)	−5.74(−1)	5.32(−1)	−2.67(−1)	5.65(−1)	−5.34(−1)

static exchange method, the present phase shifts being higher throughout the energy range considered. It may be mentioned that p-wave phase shifts are more sensitive than the d-wave predictions due to inclusion of target inelastic channels. The triplet p- and d-wave phase shifts, like s-wave, differ marginally from the static exchange predictions. On the other hand, the target elastic triplet p- and d-wave phase shifts (Sinha *et al*) are found to be sensitive like s-wave when compared with the static exchange model.

Figure 3 represents the present integrated elastic cross sections in the energy range of 0.068–100 eV along with those obtained by Sinha *et al* (1997) and Ray and Ghosh (1996, 1997). The FBA cross sections (table 4) at low incident energies are about four-fold higher than both sets of results presented here. The FBA cross sections are also higher than the

Table 3. The d-wave phase shifts in radians for [Ps(1s) + H(1s)] scattering. The numbers in parentheses indicate the power of '10'.

	Results using static exchange method		Results using three-state exchange target elastic CCA		Results using three-state exchange projectile elastic CCA	
k (au)	Singlet (η_2^+)	Triplet (η_2^-)	Singlet (η_2^+)	Triplet (η_2^-)	Singlet (η_2^+)	Triplet (η_2^-)
0.1	3.18(−5)	−3.00(−5)	3.22(−5)	−2.74(−5)	3.31(−5)	−2.83(−5)
0.2	9.17(−4)	−8.56(−4)	9.29(−4)	−7.77(−4)	9.55(−4)	−8.09(−4)
0.3	5.87(−3)	−5.37(−3)	5.96(−3)	−4.83(−3)	6.13(−3)	−5.09(−3)
0.4	1.97(−2)	−1.76(−2)	2.01(−2)	−1.55(−2)	2.06(−2)	−1.67(−2)
0.5	4.54(−2)	−3.95(−2)	4.63(−2)	−3.41(−2)	4.76(−2)	−3.76(−2)
0.6	8.09(−2)	−7.03(−2)	8.29(−2)	−5.83(−2)	8.51(−2)	−6.69(−2)
0.7	1.19(−1)	−1.06(−1)	1.23(−1)	−8.25(−2)	1.26(−1)	−1.01(−1)
0.8	1.52(−1)	−1.42(−1)	1.59(−1)	−9.71(−2)	1.61(−1)	−1.36(−1)

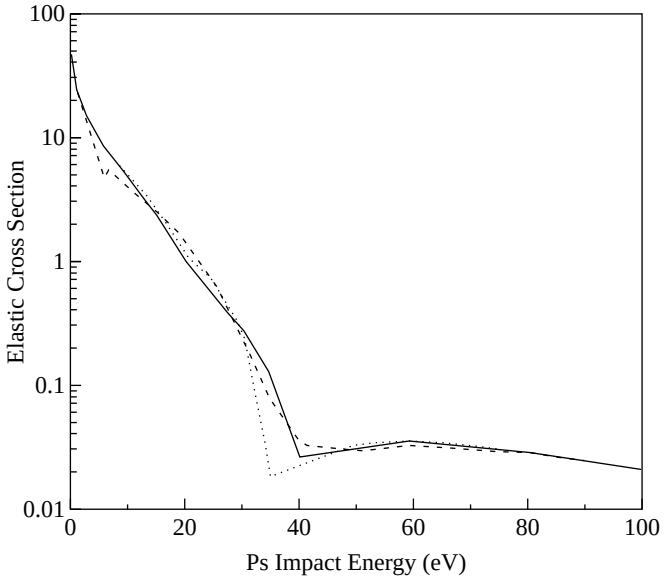

Figure 3. Elastic integrated cross section in πa_0^2. —— present results; – – – Sinha *et al* (1997); ····· static exchange, Ray and Ghosh (1997).

static exchange prediction of Ray and Ghosh (1997) (table 4) in the same order of magnitude. The kink obtained by Sinha *et al* is absent in the present calculation. There is a shallow minimum in the present results as well as in those of Sinha *et al* at about incident energy 40–45 eV. The reason for this feature is obscure. With the increase of energy, the three sets of integrated cross sections coalesce ($E \geqslant 100$ eV). At low energy up to 0.272 eV, the results of Sinha *et al*, who have applied target elastic CCA, are higher that the present prediction. In the energy range $0.612 \leqslant E < 100.0$ eV, the target elastic CCA cross sections are less than those of the present. From 100 eV onwards, two sets of results coalesce. The induced dipole interaction that arises due to the inclusion of the 2p-state of the H-atom in the present expansion scheme, influenced most significantly at the lowest energy. With the

Table 4. Integrated elastic cross sections (σ) in πa_0^2 for [H(1s) + Ps(1s)] scattering using different approximation methods. The numbers in parentheses indicate the power of '10'.

Energy (eV)	FBA exchange method	Static exchange approximation method	Three-state target elastic CCA exchange method	Three-state projectile elastic CCA exchange method
0.068	2.12(+2)	5.80(+1)	5.60(+1)	4.83(+1)
0.272	1.76(+2)	3.91(+1)	3.77(+1)	3.62(+1)
0.612	1.31(+2)	2.77(+1)	2.65(+1)	2.73(+1)
1.088	9.05(+1)	2.20(+1)	2.08(+1)	2.24(+1)
1.700	5.92(+1)	1.83(+1)	1.69(+1)	1.88(+1)
2.448	3.72(+1)	1.54(+1)	1.36(+1)	1.56(+1)
3.332	2.39(+1)	1.30(+1)	1.06(+1)	1.30(+1)
4.352	1.53(+1)	1.09(+1)	7.60(0)	1.08(+1)
5.508	9.85(0)	9.25(0)	4.88(0)	9.00(0)
6.000	8.30(0)	8.64(0)	5.67(0)	8.37(0)
6.800	6.39(0)	7.77(0)	5.57(0)	7.46(0)
10.000	2.52(0)	5.13(0)	4.06(0)	4.88(0)
15.000	6.97(−1)	2.56(0)	2.53(0)	2.29(0)
20.000	2.02(−1)	1.17(0)	1.51(0)	1.03(0)
25.000	6.17(−2)	6.88(−1)	6.96(−1)	5.27(−1)
30.000	2.70(−2)	2.91(−1)	2.42(−1)	2.81(−1)
35.000	2.37(−2)	1.89(−2)	8.03(−2)	1.19(−1)
40.000	2.80(−2)	2.30(−2)	3.41(−2)	2.66(−2)
50.000	3.55(−2)	3.36(−2)	2.94(−2)	3.19(−2)
60.000	3.67(−2)	3.61(−2)	3.34(−2)	3.57(−2)
80.000	2.99(−2)	2.99(−2)	2.93(−2)	2.99(−2)
100.000	2.18(−2)	2.18(−2)	2.18(−2)	2.18(−2)
150.000	9.65(−3)	9.65(−3)		9.64(−3)
200.000	4.77(−3)	4.76(−3)		4.76(−3)

increase of energy this effect decreases. The exchange interaction is repulsive in nature and the induced dipole interaction is attractive and long range in nature. Therefore, there is a cancellation between the two interactions. The reduction of the present integrated cross sections from the other existing theoretical predictions is thus visualized.

The present quenching cross sections and the conversion ratio are tabulated in table 5 along with those obtained by the static exchange model and the target elastic CCA. The conversion ratio is found to approach 0.25 in all the models as expected.

In table 6, we present the 1s–2s and 1s–2p excitations of hydrogen atom in which the projectile always remains in the ground state. We have also tabulated the corresponding FBA cross sections using only the exchange interaction. It may be noted that the direct FBA cross section vanishes for these processes. McAlinden *et al* tabulated target inelastic cross sections in which the projectile atom does not remain in the ground state during transitions. The present FBA and the projectile elastic CCA predictions are reported for the first time. As expected, the present CCA predictions for both the processes is less than those of the FBA. The difference between the present CCA prediction and the FBA diminishes with energy. At low energies, the contribution of $n = 2$ state excitation is appreciable when compared with elastic results.

Table 5. Quenching cross sections (σ_q) and the corresponding conversion ratios (σ_q/σ) for the [H(1s) + Ps(1s)] scattering using: (i) model 'a', the static exchange approximation method; (ii) model 'b', the three-state target elastic CCA exchange method; and (iii) model 'c', the present model, i.e. the three-state projectile elastic CCA exchange method. The numbers in parentheses indicate the power of '10'.

Energy (eV)	Quenching cross sections in πa_0^2 using			Conversion ratio using		
	Model 'a'	Model 'b'	Model 'c'	Model 'a'	Model 'b'	Model 'c'
0.068	4.50(0)	4.54(0)	2.94(0)	7.76(−2)	8.11(−2)	6.09(−2)
0.272	2.92(0)	2.98(0)	2.26(0)	7.48(−2)	7.90(−2)	6.25(−2)
0.612	2.31(0)	2.33(0)	2.10(0)	8.32(−2)	8.78(−2)	7.68(−2)
1.088	2.28(0)	2.25(0)	2.29(0)	1.04(−1)	1.09(−1)	1.02(−1)
1.700	2.18(0)	2.11(0)	2.23(0)	1.19(−1)	1.25(−1)	1.19(−1)
2.448	1.91(0)	1.80(0)	1.94(0)	1.24(−1)	1.32(−1)	1.24(−1)
3.332	1.62(0)	1.44(0)	1.62(0)	1.25(−1)	1.37(−1)	1.25(−1)
4.352	1.36(0)	1.06(0)	1.35(0)	1.24(−1)	1.41(−1)	1.25(−1)
5.508	1.15(0)	3.35(−1)	1.13(0)	1.24(−1)	6.87(−2)	1.25(−1)
6.000	1.07(0)	3.94(−1)	1.05(0)	1.24(−1)	6.95(−2)	1.25(−1)
6.800	9.61(−1)	4.59(−1)	9.42(−1)	1.24(−1)	8.25(−2)	1.26(−1)
10.000	6.29(−1)	3.98(−1)	5.95(−1)	1.22(−1)	9.79(−2)	1.22(−1)
15.000	3.07(−1)	2.55(−1)	2.78(−1)	1.20(−1)	1.01(−1)	1.21(−1)
20.000	1.35(−1)	1.53(−1)	1.14(−1)	1.15(−1)	1.01(−1)	1.11(−1)
25.000	7.13(−2)	7.02(−2)	5.50(−2)	1.04(−1)	1.01(−1)	1.04(−1)
30.000	1.86(−2)	2.42(−2)	2.86(−2)	6.39(−2)	1.00(−1)	1.02(−1)
35.000	3.31(−3)	8.89(−3)	2.14(−2)	1.76(−1)	1.11(−1)	9.77(−2)
40.000	5.63(−3)	5.39(−3)	3.30(−3)	2.46(−1)	1.58(−1)	1.24(−1)
50.000	8.39(−3)	6.92(−3)	8.09(−3)	2.50(−1)	2.37(−1)	2.53(−1)
60.000	8.94(−3)	7.92(−3)	8.89(−3)	2.48(−1)	2.41(−1)	2.49(−1)
80.000	7.41(−3)	6.91(−3)	7.41(−3)	2.48(−1)	2.42(−1)	2.48(−1)
100.000	5.42(−3)	5.09(−3)	5.42(−3)	2.48(−1)	2.43(−1)	2.48(−1)
150.000	2.39(−3)		2.40(−3)	2.50(−1)		2.50(−1)
200.000	1.17(−3)		1.19(−3)	2.50(−1)		2.50(−1)

4. Conclusion

The scattering of the Ps atom off the hydrogen target has been investigated using the projectile elastic close-coupling model having the basis sets [H(1s, 2s, 2p) + Ps(1s)] at low and medium energies. The present low-order phase shifts are compared with those obtained by static exchange as well as by target elastic CCA. The present singlet phase shifts are found to deviate from the predictions of static exchange approximation whereas the difference between the two sets of triplet phase shifts is marginal. This is due to the attractive long-range dipole interaction that arises due to the inclusion of the 2p-state of the hydrogen atom in the expansion scheme.

We report the integrated elastic, quenching cross sections in the energy range 0.068–200.0 eV. It has been found that the elastic cross sections are reduced appreciably from the static exchange predictions at low energies and the two sets of results coincide at about 100.0 eV. The conversion ratio approaches 0.25 with the increase of energy for all the models.

The 1s–2s and 1s–2p excitation cross sections of the hydrogen atom when the projectile atom always remains in the ground state have been reported for the first time. The first Born results using the exchange interaction have also been reported. The magnitude of the

Table 6. Integrated excitation cross sections in Πa_0^2 for different transitions using FBA and the present model. The numbers in parentheses indicate the power of '10'.

	Excitation cross sections for transition [H(1s)Ps(1s) => H(2s)Ps(1s)]		Excitation cross sections for transition [H(1s)Ps(1s) => H(2p)Ps(1s)]	
Energy (eV)	FBA exchange	Present CCA exchange	FBA exchange	Present CCA exchange
15.0	4.11(−1)	2.09(−1)	3.94(−1)	1.14(−1)
20.0	2.34(−1)	4.85(−1)	1.87(−1)	2.36(−1)
25.0	1.25(−1)	1.46(−1)	8.25(−2)	7.05(−1)
30.0	6.57(−2)	7.46(−2)	4.87(−2)	1.37(0)
35.0	3.43(−2)	5.81(−2)	3.85(−2)	2.25(−1)
40.0	1.79(−2)	2.12(−2)	3.45(−2)	8.51(−2)
50.0	4.92(−3)	4.92(−3)	2.85(−2)	2.85(−2)
60.0	1.48(−3)	1.47(−3)	2.23(−2)	2.12(−2)
80.0	4.57(−4)	4.76(−4)	1.27(−2)	1.21(−2)
100.0	4.32(−4)	4.48(−4)	7.24(−3)	7.06(−3)
150.0	2.93(−4)	2.97(−4)	2.30(−3)	2.23(−3)
200.0	1.65(−4)	1.66(−4)	9.54(−4)	9.37(−4)

excitation cross section is found to be appreciable with respect to the elastic one at medium energies. These excitation results will be modified if one uses the large basis set.

These low-energy results will be affected if one uses a larger basis set in the projectile elastic CCA model. Similarly the results of Sinha *et al* will also be affected with the inclusion of a large number of eigenstates or pseudostates of the Ps-atom in the expansion basis. This indicates that the excitation of both the target and the projectile atoms are to be taken into account. However, this is very complicated and requires analysis involving four angular momenta couplings. The number of coupled integral equations will be enhanced by N^2 where N is the number of integral equations to be solved for single-channel excitation and the computation labour will be huge. We hasten to add that, recently, we have performed the partial wave analysis for Ps-atom scattering in which both the atoms are allowed to be excited (Ghosh *et al* 1998).

In this calculation it is true that we have used a small basis set. However, this is the first work in which the excitation of the target atom has been considered. This prediction shows an estimate of the excitation of the target on elastic scattering. Moreover, coupled state results for the excitation of the tagged atom for Ps–atom scattering have been reported for the first time.

Acknowledgments

The authors are grateful to the Council of Scientific and Industrial Research, India, for financial support (project no 03(0758)/94/EMR-II DT 25.11.94). HR is grateful to CSIR for providing the research associateship.

References

Barker M I and Bransden B H 1968 *J. Phys. B: At. Mol. Phys.* **1** 1109
Basu M, Mukherjee M and Ghosh A S 1989 *J. Phys. B: At. Mol. Opt. Phys.* **22** 2195
Burke P G, Schey H M and Smith K 1963 *Phys. Rev.* **129** 1258

Drachman R J and Houston S K 1975 *Phys. Rev.* A **12** 885
Fraser P A 1962 *Proc. Phys. Soc.* **89** 533
Fraser P A and Kraidy M 1966 *Proc. Phys. Soc.* **89** 533
Gerner A J and Laricchia G 1996 *Can. J. Phys.* **74** 518
Ghosh A S, Sinha P K and Ray H 1998 *Nucl. Instrum. Methods* to appear
Hara S and Fraser P A 1975 *J. Phys. B: At. Mol. Phys.* **8** 1472
McAlinden M T, MacDonald F G R S and Walters H R J 1996 *Can. J. Phys.* **74** 434
Ozen, A, Garner A J and Laricchia G 1997 *Positron Workshop (Nottingham)* Book of Abstracts p 20 (poster)
Ray H and Ghosh A S 1996 *J. Phys. B: At. Mol. Opt. Phys.* **29** 5505
——1997 *J. Phys. B: At. Mol. Opt. Phys.* **30** 3745
Sarkar Nirmal K and Ghosh A S 1997 *J. Phys. B: At. Mol. Opt. Phys.* **30** 4591
Sinha Prabal K, Chaudhury Puspitapallab and Ghosh A S 1997 *J. Phys. B: At. Mol. Opt. Phys.* **30** 4644
Zafar N, Laricchia G and Charlton M 1994 *Hyperfine Interact.* **89** 243